Semiconductor Physics, Quantum Electronics & Optoelectronics, 2023. V. 26, No 2. P. 140-146.

Formation of ZnO films on SiC/porous Si/Si substrates

V.V. Kidalov[1,2], A.F. Dyadenchuk[1], V.A. Baturin[3], O.Yu. Karpenko[3], O.F. Kolomys[4], V.V. Ponomarenko[4], Z.V. Maksimenko[4], V.V. Strelchuk[4], Yu.Yu. Bacherikov[4*], O.B. Okhrimenko[4*]

[1]*Dmytro Motornyi Tavria State Agrotechnological University, 18, B. Khmelnitsky Ave., 72312 Melitopol, Ukraine*
[2]*Experimentelle Physik 2, Technische Universität Dortmund, 44221 Dortmund, Germany*
[3]*Institute of Applied Physics, NAS of Ukraine, 58, Petropavlivska str., 40030 Sumy, Ukraine*
[4]*V. Lashkaryov Institute of Semiconductor Physics, NAS of Ukraine, 41, prosp. Nauky, 03680 Kyiv, Ukraine*
[*]*Corresponding authors e-mail: olga@isp.kiev.ua; yuyu@isp.kiev.ua*

Abstract. Reactive magnetron sputtering was used to obtain ZnO films on SiC/porous Si/Si substrates. The silicon carbide film on the surface of porous Si was obtained using chemical substitution of atoms. It has been shown that ZnO films grown at the partial oxygen pressure 0.6 Pa are characterized by a smoother and more uniform surface than coatings grown at the oxygen pressure 0.1 Pa. Being based on the analysis of Raman and photoluminescence spectra, it has been shown that the increase in partial pressure of oxygen leads to the increase in structural disorder of the ZnO crystal lattice, on the one hand, and at the same time to a decrease in the concentration of intrinsic defects, including ionized oxygen vacancies O_i, on the other hand.

Keywords: reactive magnetron sputtering, porous Si, silicon carbide film, chemical substitution of atoms, Raman and photoluminescence spectra.

https://doi.org/10.15407/spqeo26.02.140
PACS 81.07.-b, 85.40.Sz

Manuscript received 01.02.23; revised version received 11.04.23; accepted for publication 07.06.23; published online 26.06.23.

1. Introduction

Zinc oxide (ZnO) is one of the most attractive materials for use in optoelectronic devices due to its wide band gap (3.37 eV) and high exciton binding energy (60 meV) [1–3]. In particular, ZnO is considered as a candidate material for use in optoelectronic devices such as ultraviolet (UV) or blue light-emitting diodes (LED) and laser diodes (LD) [4–8]. However, high-quality ZnO single crystal films are required to be used in manufacturing the high-performance LEDs. Since single crystal ZnO wafers are too expensive, most of ZnO films are produced using heteroepitaxy on foreign substrates.

The Si substrate is a very attractive material for ZnO heteroepitaxy due not only to its low cost, but also to additional advantages in the further integration of the resulting structures into photovoltaic devices. However, it is difficult to obtain high-quality monocrystalline ZnO films on Si substrates because of the large lattice mismatch between ZnO, which reaches approximately 20%; moreover, the crystal lattices of these materials are characterized by different symmetry [9]. Silicon is a cubic crystal, while ZnO has a hexagonal lattice.

The above drawbacks can be eliminated using a buffer layer with suitable structural and thermal properties in fabrication of the ZnO/Si structure. Among these materials, silicon carbide SiC is a suitable candidate. This semiconductor is attractive due to the similarity of crystal structures with ZnO and small lattice and thermal mismatch, as well as high thermal conductivity, excellent mechanical properties and good chemical stability [10]. The good lattice matching of ZnO and SiC heteroepitaxial materials allows formation of the compounds with excellent electrical and optical properties. In this case, a decrease of the compression strain in the ZnO film will also lead to a decrease in the crystallite size [11]. However, the commercial cost of manufacturing of single crystal SiC films is also very high. The solution of this problem was creation of single-crystal SiC films with a low dislocation density on the surface of Si wafers. The Si substrate can be successfully used to further reduce the cost of manufacturing large area SiC films.

It is also an advantage that when using Si as substrate, for example for fabrication of GaN- or ZnO-based LEDs, the films can be compatible and integrated to form all Si-based optoelectronic devices. To obtain SiC films on single-crystal silicon substrates, a nanoporous Si layer can be used, which plays the role of a soft substrate and adjusts to the structure of the SiC film, reducing mechanical stresses caused by the lattice mismatch between SiC and Si [12].

© V. Lashkaryov Institute of Semiconductor Physics of the NAS of Ukraine, 2023
© Publisher PH "Akademperiodyka" of the NAS of Ukraine, 2023

A silicon carbide film can be obtained by chemical substitution of atoms [12, 13], which enables to successfully combine the advantages of both silicon carbide and silicon, and to obtain thin films of monocrystalline SiC on Si substrates in relatively low-temperature processes (1200…1350 °C) that do not require large energy costs. A distinctive feature of this method is that the silicon carbide film is formed directly in the near-surface bulk of the substrate and from its material – silicon – by substituting some of the Si atoms for C [13].

This work is devoted to the study of properties inherent to the zinc oxide films prepared using magnetron sputtering on a SiC/porous Si/Si template.

2. Experimental technique

Micro Raman scattering (Raman) and photoluminescence (PL) spectra of ZnO were recorded using a Horiba Jobin Yvon T64000 triple spectrometer with an Olympus BX41 confocal microscope (×50 objective, aperture 0.75). Micro Raman spectra were measured in backscattering geometry. To excite the Raman spectra, radiation from a Spectra Physics Excelsior DPSS laser with the wavelength λ_{ex} = 532.0 nm was used; for excitation of the PL spectra, radiation from a He–Cd laser with the wavelength λ_{ex} = 325.0 nm was used. SEM images of the ZnO/SiC/porous Si/Si structures were obtained using a Tescan Mira 3 LMU scanning electron microscope.

Method for obtaining the ZnO/SiC/porous Si/Si structure

Monocrystalline silicon plates were used as a base for the SiC/porous Si/Si multilayer substrate. The plate diameter was 100 mm, thickness – 460 ± 25 µm, electrical resistivity – 1...10 Ohm·cm, operating side of plates was polished, reverse side was grinding-etched, dislocation density <100 cm^{-2}.

The process of electrochemical etching of Si(100) plates for obtaining a porous Si layer consisted of the following three stages.

The stage 1 – pre-cleaning. Before the etching procedure, the following steps were performed to prepare monocrystalline Si(100) plates:

- grinding the samples with diamond paste;
- cleaning of plates with toluene, ethanol and isopropanol;
- washing in running deionized water (removal of pretreatment reaction products);
- drying of the plates by using a centrifuge in a jet of purified dry air.

The stage 2 – actual etching process.

The electrolyte $HF:H_2O:C_2H_5OH$ = 2:1:1 (40% hydrofluoric acid, 96% alcohol) was used in the experiment. A platinum plate with the dimensions 5×10×1 mm was used as a cathode, which was located 2...3 cm away from the semiconductor electrode (anode). The current density was 50 mA/cm^2, and the duration of the etching process – 1200 s. A DC power supply (30 V, 10 A) was used as a power source.

The stage 3 – cleaning of the processed plates from etching products. After electrochemical treatment, the obtained samples were dried in a flow of a mixture of hydrogen, nitrogen, and hot air.

The SiC film was deposited on a porous Si/Si substrate by using the atom substitution method [12, 13]. Directly before annealing, the air from the chamber was evacuated using a 2NVR-5DM rotary pump to a pressure of 10^{-2} to 10^{-3} Pa. The porous Si/Si sample placed into the setup was heated by a graphite heater to a temperature of 950 to 1350 °C. Then, using the HORIBA gas regulator, CO and SiH_4 gases were pumped through the connecting gas pipes, the total pressure of the CO + SiH_4 gas mixture was 133 Pa, CO and SiH_4 gas flows were 14 and 3.5 cm^3/min, respectively. The total pressure in the reaction zone was maintained within 20...600 Pa. The duration of the synthesis process was 20...60 min.

Technological conditions for the synthesis of SiC layers on samples of porous-Si/Si (100) are listed in Table 1.

After formation of the SiC/porous Si/Si substrate, ZnO films were deposited onto the SiC surface. Deposition of ZnO films was performed by reactive high frequency magnetron sputtering of a zinc target. For deposition of ZnO films, the substrates were fixed using special clamps that carried out their movement inside the vacuum chamber. The substrates and target were placed in parallel to each other. The target for zinc oxide sputtering was a zinc disc of 80 mm in diameter and 6-mm thick, with 5N purity. During the growth of zinc oxide, argon (99.9995%) and oxygen (99.9995%) entered the operating chamber.

Table 1. Conditions for the synthesis of SiC layers on samples of porous Si/Si (100).

Parameter	Value
Temperature of growth, °C	1290
Time of growth, min	30
Total pressure of the CO + SiH_4 gas mixture, Pa	133
CO gas flow, cm^3/min	14
SiH_4 gas flow, cm^3/min	3.5

Table 2. Parameters of the process of ZnO films deposition.

Parameter	Value
Residual pressure in the vacuum chamber, Pa	10^{-3}
Pressure of oxygen P_{O2}, Pa	0.1
Pressure of argon P_{Ar}, Pa	1
Temperature of substrate, °C	300
Power on the discharge of the RF magnetron, W	200
Distance target-substrate, m	0.07
Time of deposition, s	1200

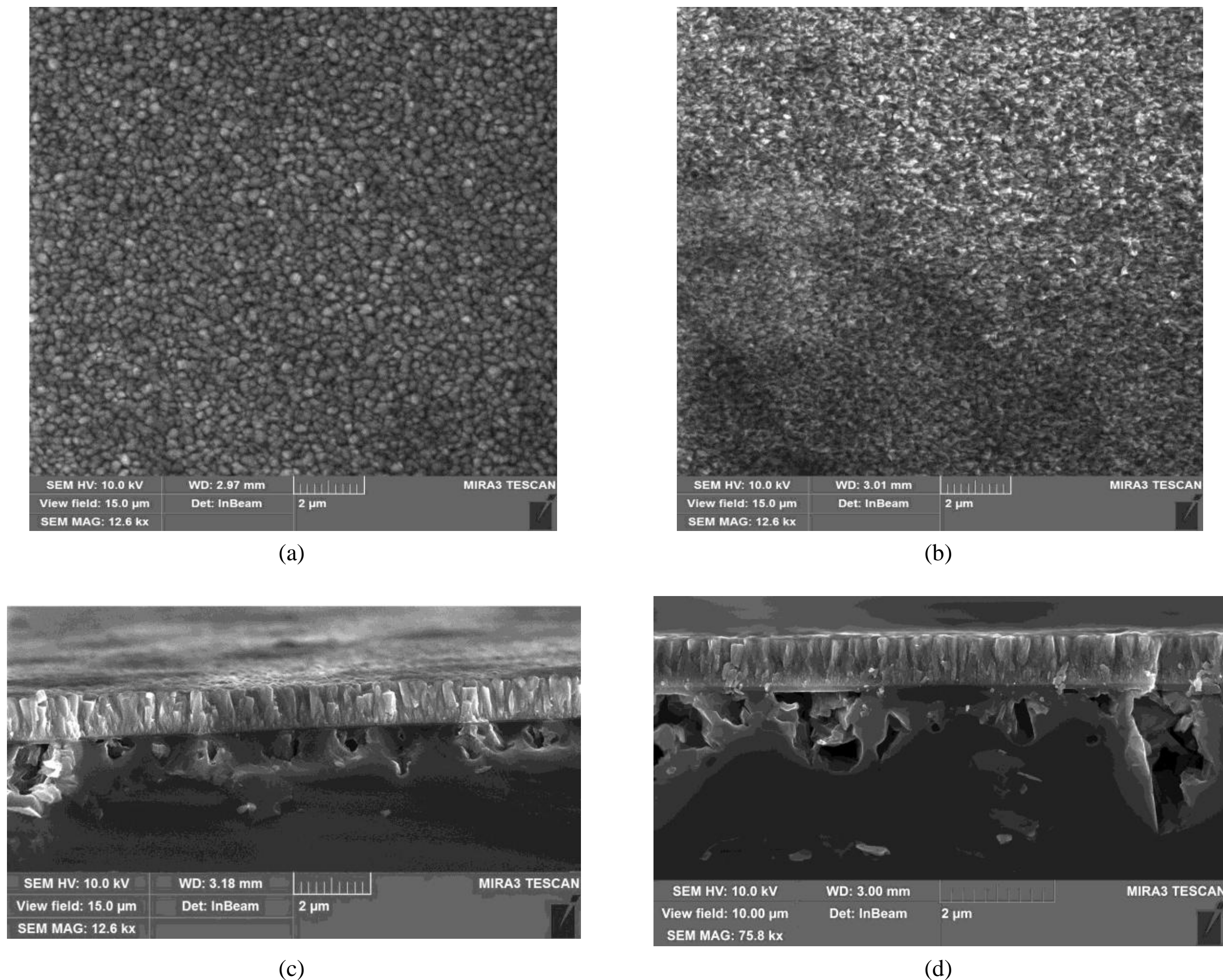

Fig. 1. SEM images of the surface (a, c) and cleavage (b, d) of ZnO films grown on SiC/porous Si/Si substrates prepared at the oxygen pressure 0.1 and 0.6 Pa, respectively.

The parameters of the process of deposition of ZnO films by the method of magnetron sputtering of a zinc target are shown in Table 2.

3. Results and discussion

3.1. Morphological studies

Fig. 1 shows the SEM images of the surface and cleavage of ZnO films grown on SiC/porous Si/Si substrates prepared at the oxygen pressure values 0.1 and 0.6 Pa.

As can be seen in Fig. 1, the ZnO film prepared at the oxygen pressure 0.6 Pa has a smoother surface than those at the pressure 0.1 Pa. In both cases, a columnar structure typical for ZnO films is observed on the surface of the samples. In this case, the high packing density leads to coalescence of individual crystallites. With increasing the pressure, the thickness of the ZnO film somewhat decreases from 1108 nm at 0.1 Pa to 864 nm at 0.6 Pa. The decrease of the thickness of ZnO film is caused by a decrease in the film deposition rate with an increase in the partial pressure of oxygen, which is typical for the method of magnetron sputtering of films [14].

3.2. Raman spectroscopy

Raman scattering (RS) was used to study the structural perfection and phonon properties of ZnO films deposited by magnetron sputtering on SiC/porous Si/Si substrates.

According to the group-theoretical analysis, optical phonons of ZnO are described by irreducible representations at the center of the Brillouin zone: $\Gamma_{opt} = A_1 + 2B_1 + E_1 + 2E_2$ [15]. Polar A_1 and E_1 phonon vibrations are split into longitudinal optical (LO) and transverse optical (TO) phonon modes that manifest themselves in Raman and infrared (IR) spectra. Inelastic scattering by E_2 (high) and E_2 (low) phonon vibrations is allowed in Raman spectra, while the scattering by vibrations of B_1 symmetry (silent modes) is forbidden and does not manifest in the optical spectra of structurally perfect crystals.

Fig. 2 shows the Raman spectra of ZnO films grown on SiC/porous Si/Si substrates under different oxygen partial pressures. The Raman spectra of all the samples contain Raman bands marked with the symbol * at 303, 442, 521, 620, 671, 826, and 944 ... 980 cm^{-1}, corresponding to the Raman bands of the first and second

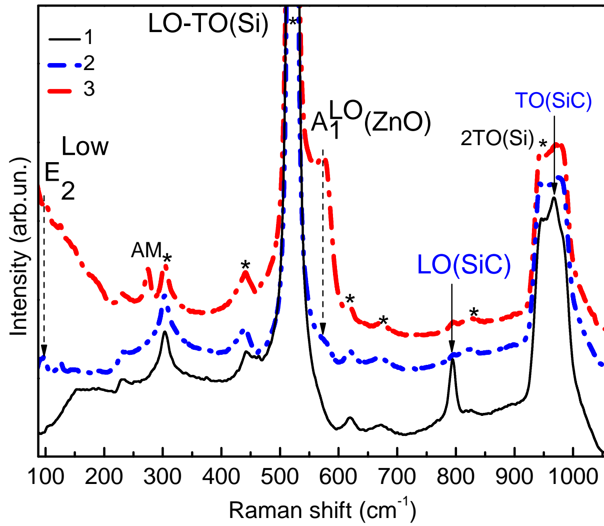

Fig. 2. Raman spectra of the SiC/porous Si/Si substrate (*1*) and ZnO films grown under the pressure 0.1 Pa (*2*) and 0.6 Pa (*3*) on a SiC/porous Si/Si substrate. The symbol * denotes the Raman bands of the Si substrate (λ_{ex} = 532.0 nm, T = 300 K).

orders in the Si substrate [16]. The Raman bands at 795 and 967 cm^{-1} are caused by scattering related to LO and TO phonons of the layer of cubic 3C-SiC modification, respectively [17].

The Raman spectra of ZnO/SiC/porous Si/Si (Fig. 2, curves *2* and *3*) measure a band at 574 cm^{-1} corresponding to the scattering by A_1(LO) phonons of ZnO. The relatively high intensity of the band in the non-resonant Raman spectra of ZnO films can be explained as a result of the defect-induced inelastic scattering. With an increase in the concentration of structural defects, an increase in the structural disordering of the ZnO crystal lattice takes place, which manifests itself in the Raman spectra in an increase in the intensity of polar A_1(LO) mode and the practical absence of non-polar E_2 (low) and E_2 (high) phonon modes (Fig. 2). As it was shown by the authors of [18], the appearance of an ensemble of randomly oriented nanowires or columns that are characteristic of the ZnO structure (see Fig. 1) can lead to an increase in the intensity of polar A_1(LO) mode. In this case, the increase in the intensity of the A_1(LO) mode with respect to the non-polar E_2(low) and E_2(high) phonon modes is due to such effects as deformation and disordering in the ensemble of ZnO nanowires. With an increase in the partial pressure of oxygen, the intensity of the A_1(LO) mode in the Raman spectra increases (Fig. 2). This may be due to the fact that with a decrease of the film thickness observed with increasing the partial oxygen pressure (Fig. 1), the contribution of disordering effects as well as the reflection of exciting radiation at the boundaries between the individual columns are increased.

In the Raman spectrum of ZnO film grown under the oxygen pressure 0.6 Pa, an additional band is found at ~275.0 cm^{-1}, which cannot be associated with the process of inelastic scattering of the first or second order by phonons of wurtzite ZnO. To date, the nature of this band remains unclear. In [19], a linear correlation was found between the nitrogen concentration and the intensity of vibrational bands at 275.0 and 582.0 cm^{-1}, which allowed the authors to interpret these bands as local vibrations involving nitrogen. An increase in the intensity of the 275 cm^{-1} band during thermal annealing [20] associated with vibrations of Zn atoms in the local environment, where some of the nearest neighboring oxygen atoms substitute nitrogen atoms in the ZnO lattice [21]. It is assumed in [22] that the additional modes can be caused by the effects of disordering of the ZnO crystal lattice and do not depend on the features of incorporation of nitrogen atoms into the ZnO matrix.

To confirm this assumption, they carried out polarization Raman studies of ZnO films doped with Fe, Sb, Al, Ga, and Li grown on a sapphire substrate by using the method of pulsed laser sputtering. Thus, additional modes at 277, 511, 583, and 644 cm^{-1} were recorded in the Raman spectra of ZnO films doped with Fe, Sb, and Al. In [23], this additional band was assigned to a local vibrational mode in the Raman spectra of clusters formed by interstitial zinc Zn_i. In addition, the marked band may correspond to the B_1(low) ZnO mode. A high level of impurities or structural defects leads to a weakening of the selection rules for the Raman scattering, and registration of this “forbidden” band becomes possible.

3.3. Photoluminescent research

Fig. 3 shows room-temperature PL spectra of ZnO films grown on a SiC/porous Si/Si substrate at various values of oxygen partial pressure, as well as the PL spectrum of the SiC/porous Si/Si substrate. The PL spectra of both structures contain intense emission bands, both in the ultraviolet and visible spectral ranges.

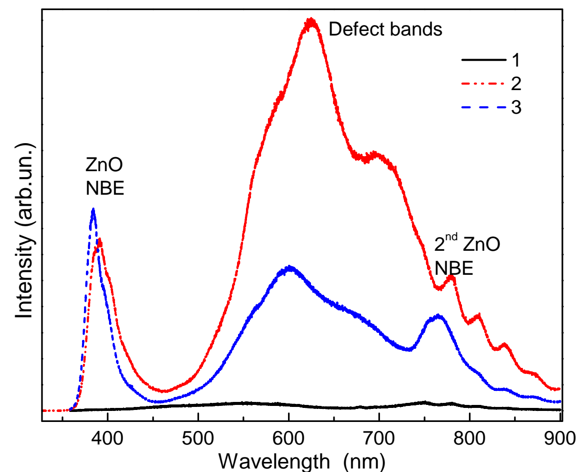

Fig. 3. PL spectra of the SiC/porous Si/Si substrate (*1*) and ZnO films grown under the pressure 0.1 Pa (*2*) and 0.6 Pa (*3*) on the SiC/porous Si/Si substrate. T = 300 K, λ_{exc} = 325 nm.

The PL spectrum of the ZnO film (Fig. 3, curves *2* and *3*) with interband excitation λ_{exc} = 325 nm (E_{ex} = 3.81 eV) contains an intense ultraviolet near-band-edge (NBE) emission band with a maximum at ~383 nm for the case when the film was grown at the oxygen pressure 0.6 Pa and 388 nm for the case of the oxygen pressure 0.1 Pa, which is caused by the radiative recombination of free excitons [24]. The shape of this PL band has a low-energy asymmetry, which indicates the efficiency of radiative recombination processes involving longitudinal optical phonons [24]. The difference in the positions of the maxima inherent to the edge PL band in ZnO films at different pressures, as compared to bulk ZnO (368 nm) [25], is caused by the presence of elastic deformations through the mismatch between the lattice constants and thermal expansion coefficients of the film and substrate [26].

The broad emission band with the maxima at 560, 625 and 700 nm is associated with radiative processes that occur at deep energy levels in the band gap and are caused by various types of intrinsic defects, including ionized oxygen vacancies O_i [27, 28]. The decrease in the intensity of this emission band in the PL spectra of ZnO/SiC/porous Si/Si with an increase in the partial pressure of oxygen indicates a decrease in the concentration of intrinsic defects.

4. Conclusions

Thus, as a result of the studies of ZnO films grown on the SiC/porous Si/Si substrate by applying the magnetron RF sputtering, it has been shown that ZnO films grown under the oxygen pressure 0.6 Pa are characterized by a smoother and more uniform surface than those obtained under the oxygen pressure 0.1 Pa. It has been found that the prepared ZnO films have the thickness close to 1108 nm (at 0.1 Pa) and 864 nm (at 0.6 Pa).

It has been shown that, with an increase in the oxygen partial pressure, the intensity of the A_1(LO) mode (574 cm^{-1}) in the Raman spectrum of the ZnO/SiC/porous Si/Si structure increases, which indicates an increase in the structural disordering in the columnar structure of the ZnO film. At the same time, with an increase in the partial pressure of oxygen, the intensity of the broad emission band with the maxima at 560, 625, and 700 nm in the PL spectra of ZnO/SiC/porous Si/Si decreases, which indicates a decrease in the concentration of intrinsic defects, including ionized oxygen vacancies O_i.

Acknowledgement

The study was supported by the Ministry of Education and Science of Ukraine (№ 0121U113502).

References

1. Mele P. (Ed.). *ZnO Thin Films: Properties, Performance and Applications*. Nova Science Pub Inc, New York, 2019.
2. Vyas S. A short review on properties and applications of zinc oxide based thin films and devices: ZnO as a promising material for applications in electronics, optoelectronics, biomedical and sensors. *Johnson Matthey Technol. Rev*. 2020. **64**, Issue 2. P. 202–218. https://doi.org/10.1595/205651320X15694993568524.
3. Zahoor R., Jalil A., Ilyas S.Z. *et al*. Optoelectronic and solar cell applications of ZnO nanostructures. *Results in Surfaces and Interfaces*. 2021. **2**. P. 100003. https://doi.org/10.1016/j.rsurfi.2021.100003.
4. Roy A., Benhaliliba M. Investigation of ZnO/*p*-Si heterojunction solar cell: Showcasing experimental and simulation study. *Optik*. 2023. **274**. P. 170557. https://doi.org/10.1016/j.ijleo.2023.170557.
5. Ilican S., Gorgun K., Aksoy S. *et al*. Fabrication of *p*-Si/*n*-ZnO:Al heterojunction diode and determination of electrical parameters. *J. Mol. Struct*. 2017. **1156**. P. 675–683. https://doi.org/10.1016/j.molstruc.2017.11.121.
6. Mitta S.B., Murahari P., Nandanapalli K.R. *et al*. Si/ZnO heterostructures for efficient diode and water-splitting applications. *Int. J. Hydrog. Energy*. 2018. **43**. P. 16015–16023. https://doi.org/10.1016/j.ijhydene.2018.07.038.
7. Rahman F. Zinc oxide light-emitting diodes: a review. *Opt. Eng*. 2019. **58**, Issue 1. P. 010901. https://doi.org/10.1117/1.OE.58.1.010901.
8. Jangir L.K., Kumari Y. and Kumari P. Zinc oxide-based light-emitting diodes and lasers. In: *Nanostructured Zinc Oxide Synthesis, Properties and Applications, Metal Oxides*. Elsevier, Amsterdam. 2021. P. 351–374. https://doi.org/10.1016/B978-0-12-818900-9.00010-3.
9. Gupta C.P., Singh A.K., Birla S. *et al.* Ultraviolet light detection properties of ZnO/AlN/Si heterojunction diodes. *J. Electron. Mater.* 2022. **51**. P. 1097–1105. https://doi.org/10.1007/s11664-021-09374-w.
10. Kimoto T., Cooper J.A. *Fundamentals of Silicon Carbide Technology: Growth, Characterization, Devices and Applications*. Wiley-IEEE Press, 2014. https://doi.org/10.1002/9781118313534.
11. Ghosh T., Dutta M., Basak D. Effect of substrate-induced strain on the morphological, electrical, optical and photoconductive properties of RF magnetron sputtered ZnO thin films. *Mater. Res. Bulletin*. 2011. **46**. P. 1039–1044. http://dx.doi.org/10.1016/j.materresbull.2011.03.011.
12. Kidalov V.V., Kukushkin S.A., Osipov A.V. *et al*. Heteroepitaxy growth of SiC on the substrates of porous Si method of substitution of atoms. *J. Nano- Electron. Phys*. 2018. **10**. P. 03026. https://doi.org/10.21272/jnep.10(3).03026.
13. Kukushkin S.A., Osipov A.V. Drift mechanism of mass transfer on heterogeneous reaction in crystalline silicon substrate. *Phys. B: Condens. Matter.* 2017. **512**. P. 26–31. https://doi.org/10.1016/j.physb.2017.02.018.

14. Chen J.J., Gao Y., Zeng F. *et al*. Effect of sputtering oxygen partial pressures on structure and physical properties of high resistivity ZnO films. *Appl. Surf. Sci.* 2004. **223**. P. 318–329. https://doi.org/10.1016/j.apsusc.2003.09.015.
15. Damen T.C., Porto S.P.S., Tell B. Raman effect in zinc oxide. *Phys. Rev*. 1966. **142**. P. 570–574. https://doi.org/10.1103/PhysRev.142.570.
16. Wolf I.D. Micro-Raman spectroscopy to study local mechanical stress in silicon integrated circuits. *Semicond. Sci. Technol*. 1996. **11**, Issue 2. P. 139–154. https://doi.org/10.1088/0268-1242/11/2/001.
17. Rohmfeld S., Hundhausen M., Ley L. *et al.* Quantitative evaluation of biaxial strain in epitaxial 3C-SiC layers on Si(100) substrates by Raman spectroscopy. *J. Appl. Phys*. 2002. **91**, Issue 3. P. 1113–1117. https://doi.org/10.1063/1.1427408.
18. Alarcón-Lladó E., Ibáñez J., Cuscó R. *et al*. Ultra-violet Raman scattering in ZnO nanowires: quasi-mode mixing and temperature effects. *J. Raman Spectrosc*. 2011. **42**. P. 153–159. https://doi.org/10.1002/jrs.2664.
19. Kaschner A., Haboeck U., Strassburg M. *et al.* Nitrogen-related local vibrational modes in ZnO:N. *Appl. Phys. Lett*. 2002. **80**. P. 1909. https://doi.org/10.1063/1.1461903.
20. Zhu X., Wu H., Yuan Z. *et al.* Multiphonon resonant Raman scattering in N-doped ZnO. *J. Raman Spectrosc*. 2009. **40**. P. 2155–2161. https://doi.org/10.1002/jrs.2385.
21. Wang J.B., Zhong H.M., Li Z.F., Lu W. Raman study of N^+-implanted ZnO. *Appl. Phys. Lett*. 2006. **88**. P. 101913. https://doi.org/10.1063/1.2185261.
22. Bundesmann C., Ashkenov N., Schubert M. *et al*. Raman scattering in ZnO thin films doped with Fe, Sb, Al, Ga, and Li. *Appl. Phys. Lett*. 2003. **83**. P. 1974. https://doi.org/10.1063/1.1609251.
23. Gluba M.A., Nickel N.H., Karpensky N. Interstitial zinc clusters in zinc oxide. *Phys. Rev. B*. 2013. **88**. P. 245201. https://doi.org/10.1103/PhysRevB.88.245201.
24. Chen Y.W., Liu Y.C., Lu S.X. *et al.* Optical properties of ZnO and ZnO:In nanorods assembled by sol-gel method. *J. Chem. Phys*. 2005. **123**. P. 134701. https://doi.org/10.1063/1.2009731.
25. Meyer B.K., Alves H., Hofmann D.M. *et al*. Bound exciton and donor-acceptor pair recombinations in ZnO. *phys. status solidi (b)*. 2004. **241**. P. 231–260. https://doi.org/10.1002/pssb.200301962.
26. Singh J., Ranwa S., Akhtar J., Kumar M. Growth of residual stress-free ZnO films on SiO_2/Si substrate at room temperature for MEMS devices. *AIP Adv*. 2015. **5**. P. 067140. https://doi.org/10.1063/1.4922911.
27. Leiter F., Alves H., Pfisterer D. *et al.* Oxygen vacancies in ZnO. *Phys. B*. 2003. **340**. P. 201. https://doi.org/10.1016/j.physb.2003.09.031.
28. Galdámez-Martinez A., Santana G., Güell F. *et al.* Photoluminescence of ZnO nanowires: A review. *Nanomaterials*. 2020. **10**. P. 857. https://doi.org/10.3390/nano10050857.

Authors and CV

Valeriy V. Kidalov, defended his Doctoral Dissertation in Physics and Mathematics in 2004. Doctor of Physical and Mathematical Sciences, Professor, Dmytro Motornyi Tavria State Agrotechnological University. Authored over 250 publications, 8 patents, 3 monographs. The area of his scientific interests includes new phase nucleation on the surface, in particular, nucleation of thin films, nanostructures and quantum dots.
https://orcid.org/0000-0002-5128-1880

Alena F. Dyadenchuk, Candidate of Technical Sciences since 2018. Associate Professor of the Department of Higher Mathematics and Physics of Dmytro Motornyi Tavria State Agrotechnological University. Authored about 100 publications, 12 patents, 2 monographs. The area of her scientific interests includes the manufacture of nanostructured materials and the study of their properties, as well as heterostructures based on porous semiconductors. https://orcid.org/0000-0002-6625-9985

Volodymyr A. Baturin, Member of Academic Council, Principal research assistant, Deputy head of the Department, Head of the Laboratory at the Institute of Applied Physics, NAS of Ukraine. The area of scientific interests includes the manufacture of nanostructured materials, physics of nuclei, elementary particles and high energies. https://orcid.org/0000-0001-6171-8575

Oleksandr Yu. Karpenko, Junior researcher of the Institute of Applied Physics, NAS of Ukraine. Author of more than 40 publications, 2 patents. Research interests include the influence of surface modification on the probability of high-vacuum breakdown, technology of thin films, ion implantation.
https://orcid.org/0000-0001-9280-082X

Valentyna V. Ponomarenko, scientific researcher at the V. Lashkaryov Institute of Semiconductor Physics, NAS of Ukraine. Candidate for the degree of PhD. Authored 5 papers and 2 theses. The area of her scientific interests is properties of functional materials.
E-mail: freundlich@ukr.ne,
https://orcid.org/0000-0001-5722-9760

Oleksandr F. Kolomys, PhD, Senior Researcher at the Laboratory of submicron optical spectroscopy at the V. Lashkaryov Institute of Semiconductor Physics, NASU. Authored over 130 publications, 3 patents, 3 chapters of textbooks. The area of his scientific interests includes Raman and luminescent microanalysis of light emitting properties, structure, composition, electronic and phonon excitations in solids, physical and chemical properties of semiconductors, chemicals and nanostructures with submicron spatial resolution.
E-mail: olkolomys@gmail.com,
https://orcid.org/0000-0002-1902-4075

Viktor V. Strelchuk, defended his Doctoral Dissertation in Physics and Mathematics in 2006 and became full professor in 2016. Professor at the Laboratory of submicron optical spectroscopy, V. Lashkaryov Institute of Semiconductor Physics, NASU. Authored over 300 publications, 10 patents, 6 textbooks. The area of his scientific interests includes optical spectroscopy of low-dimension structures, technology, physics and applications of semiconductors and their nanostructures, confocal Raman spectroscopy, FTIR. https://orcid.org/0000-0002-6894-1742.
E-mail: viktor.strelchuk@ccu-semicond.net

Zoya V. Maksimenko, PhD in Physics and Mathematics, Researcher at the Department of Structural and Elemental Analysis of Materials and Systems at the V. Lashkaryov Institute of Semiconductor Physics. The main direction of her scientific activity is studying the semiconductor nanostructures by using high-resolution X-ray diffractometry in the field of anomalous X-ray dispersion.
E-mail: ZMaksimenko@gmail.com,
https://orcid.org/0000-0002-3434-3728

Yuriy Yu. Bacherikov, Doctor of Science in Physics and Mathematics, Leading scientific collaborator at the V. Lashkaryov Institute of Semiconductor Physics, NASU. Authored over 300 publications, 6 patents, 1 monograph. The area of his scientific interests includes physics and applications of wide-band semiconductor compounds and devices based on them.
https://orcid.org/0000-0002-9144-4592

Olga B. Okhrimenko, Doctor of Science in Physics and Mathematics, Leading scientific collaborator at the V. Lashkaryov Institute of Semiconductor Physics, NASU. Authored over 140 publications, 1 patent, 1 monograph. The area of her scientific interests includes investigation of the patterns and physical mechanisms of formation and rearrangement of the defect-impurity system in the thin-film dielectric-semiconductor structures. https://orcid.org/0000-0002-7611-4464

Authors' contributions

Kidalov V.V.: resources, conceptualization, supervision, project administration.
Dyadenchuk A.F.: sample preparation, manufacture of substrate, investigation.
Baturin V.A.: sample preparation, thin films ion implantation.
Karpenko O.Yu.: sample preparation, manufacture of ZnO films.
Kolomys O.F.: performed experiments of Raman and luminescent microanalysis, analyzing the data.
Strelchuk V.V.: validation, investigation Raman and luminescent experimental data.
Ponomarenko V.V.: investigation.
Maksimenko Z.V.: visualization, verification, editing.
Bacherikov Yu.Yu.: key ideas, conceptualization, investigation, writing – review & editing.
Okhrimenko O.B.: key ideas, conceptualization, investigation, writing – original draft, supervision.

Формування плівок ZnO на підкладках SiC/пористий Si/Si

В.В. Кідалов, А.А. Дяденчук, В.А. Батурін, О.Ю. Карпенко, О.Ф. Коломис, В.В. Пономаренко, З.В. Максименко, В.В. Стрельчук, Ю.Ю. Бачеріков, О.Б. Охріменко

Анотація. Методом реактивного магнетронного напилення одержано плівки ZnO на підкладках SiC/пористий Si/Si. При цьому плівка карбіду кремнію на поверхні пористого Si була отримана методом хімічного заміщення атомів. Показано, що плівки ZnO, вирощені при парціальному тиску кисню 0.6 Па, характеризуються більш гладкою та однорідною поверхнею, ніж покриття, отримані при тиску кисню 0.1 Па. На підставі аналізу спектрів раманівського розсіяння світла та фотолюмінесценції показано, що збільшення парціального тиску кисню приводить до збільшення структурного розупорядкування кристалічної ґратки ZnO з одного боку, і в той же час до зменшення концентрації власних дефектів, у тому числі іонізованих кисневих вакансій O_i, з іншого боку.

Ключові слова: реактивне магнетронне напилення, пористий Si, плівка карбіду кремнію, метод хімічного заміщення атомів, спектри раманівського розсіяння світла та фотолюмінесценції.